

# Calcium Modification of Spinel Inclusions in Aluminum-Killed Steel: Reaction Steps

NEERAV VERMA, PETRUS C. PISTORIUS, RICHARD J. FRUEHAN,  
MICHAEL S. POTTER, HELMUT G. OLTMANN, and EUGENE B. PRETORIUS

Calcium treatment is a well-established way to modify solid alumina inclusions to liquid or partially liquid calcium aluminates. Spinel ( $\text{Al}_2\text{O}_3 \cdot x\text{MgO}$ ) can also form in liquid steel after aluminum deoxidation. Like alumina, the spinels can be modified readily to liquid inclusions by a calcium treatment. The modification of spinels was studied by observing the transient evolution of inclusions, in laboratory and industrial heats. Spinel modification involves the preferential reduction of MgO from the spinel, with Mg dissolving in the steel, and it proceeds through transient calcium sulfide formation, just like in the case of alumina inclusions. Because magnesium dissolves in steel after the calcium treatment of spinels, the reoxidation of the melt will produce new spinels.

DOI: 10.1007/s11663-012-9660-4

© The Minerals, Metals & Materials Society and ASM International 2012

## I. INTRODUCTION

### A. Origin of Spinel Inclusions in Aluminum-Killed, Low-Carbon Steel

MAGNESIUM spinel inclusions (solid solutions of  $\text{MgAl}_2\text{O}_4$  and  $\text{Al}_2\text{O}_3$ ) form in aluminum-killed steels during secondary metallurgy, if the ladle slag is well deoxidized (with low FeO and MnO levels)<sup>[1]</sup>; arcing during ladle furnace processing also contributes to the spinel formation.<sup>[2]</sup> Spinel inclusions seem to form in liquid steel mainly by a reaction between the liquid steel and the ladle slag (rather than by reaction between steel and refractory); this conclusion is supported by the following recently reported observations: (1) The magnesium oxide content in inclusions increases in parallel with silicon pickup by the steel (and silicon pickup occurs by reaction between steel and ladle slag)<sup>[3]</sup>; (2) no difference in spinel formation was found in steel contained in ladles fully lined with MgO-C brick, and ladles with MgO-C at the slag line only<sup>[4]</sup>; and (3) reaction between aluminum-killed steel and an MgO crucible (in laboratory runs) did yield spinel as product, but the spinel particles remained at the steel-MgO interface and did not enter the steel melt.<sup>[5]</sup>

### B. Calcium Modification of Spinel Inclusions

It is now well established that the spinels in the liquid steel are modified readily to liquid inclusions, fully or partially, through calcium treatment.<sup>[3,5,6]</sup> Important differences between the calcium modification of alumina and of spinel inclusions are as follows: (1) Liquid oxide is the first product when calcium reacts with spinel, whereas the solid calcium aluminates form first when the calcium reacts with alumina (for this reason it has been suggested that spinels are easier to modify than alumina)<sup>[7]</sup> and (2) the modification of spinels involves a decrease in the MgO content of the inclusions.<sup>[3]</sup> Figure 1 shows an example of the latter effect. In this figure, the inclusion compositions are plotted on a Mg-Al-Ca diagram; the area of each symbol is proportional to the number fraction of inclusions with that composition.<sup>[8]</sup> The observed decrease in MgO (as in Figure 1) is real and not an artifact of matrix effects during microanalysis of these micron-sized inclusions<sup>[9]</sup>; magnesium dissolves in the liquid steel after calcium treatment.<sup>[3]</sup>

Although the MgO content of the inclusions decreases after calcium treatment, even small percentages of MgO remaining in the inclusions can contribute significantly to liquefaction of the inclusions and so promote castability.<sup>[3]</sup> The effect of small MgO percentages is illustrated in Figure 2, which gives the mass percentage of liquid in  $\text{Al}_2\text{O}_3$ -CaO-MgO inclusions with different mass ratios of Ca to O in the inclusions (higher Ca:O ratios correspond to greater degrees of modification). Clearly, even at lower Ca:O ratios (0.6 or less) which give no liquefaction in binary CaO- $\text{Al}_2\text{O}_3$  inclusions, the presence of even a small fraction of MgO in the inclusions greatly increases the proportion of liquid. For example, Figure 2 shows that a Mg cation fraction – the molar ratio  $\text{Mg}/(\text{Mg} + \text{Ca} + \text{Al})$  in the inclusion – of 0.025 is sufficient to give 100% liquid in  $\text{Al}_2\text{O}_3$ -CaO-MgO inclusions with a Ca:O mass ratio of 0.6, whereas inclusions with the same Ca:O mass ratio would be fully

NEERAV VERMA, formerly PhD Candidate, with the Center for Iron and Steelmaking Research (CISR), Department of Materials Science and Engineering, Carnegie Mellon University, Pittsburgh, PA 15213, and is now Research Engineer, with ExxonMobil Upstream Research Company, Houston, TX 77098. PETRUS C. PISTORIUS and RICHARD J. FRUEHAN, Professors, are with the Center for Iron and Steelmaking Research (CISR), Department of Materials Science and Engineering, Carnegie Mellon University. Contact e-mail: pistorius@cmu.edu MICHAEL S. POTTER, Scientist, is with the RJ Lee Group, Monroeville, PA 15146. HELMUT G. OLTMANN, LMF/VTD Metallurgist, is with Nucor Steel, Mount Pleasant, SC 29465. EUGENE B. PRETORIUS, Manager, is with Steelmaking Technology, Nucor Steel, Mount Pleasant, SC 29465.

Manuscript submitted January 17, 2012.

Article published online October 4, 2012.

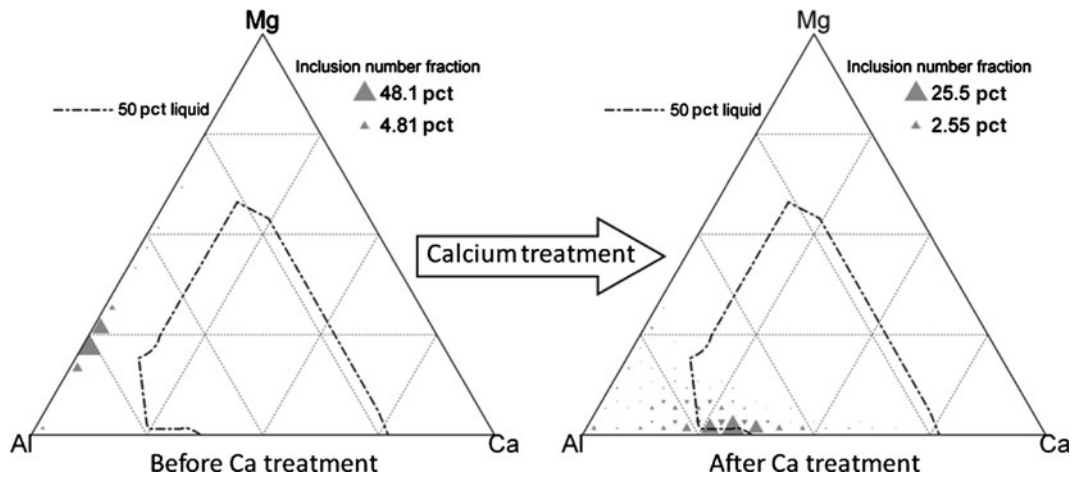


Fig. 1—Change in inclusion composition after calcium treatment, for a laboratory heat deoxidized with 65 pct Al-35 pct Mg alloy and then calcium treated. Inclusion compositions plotted on Al-Mg-Ca ternary diagram (mole fractions).

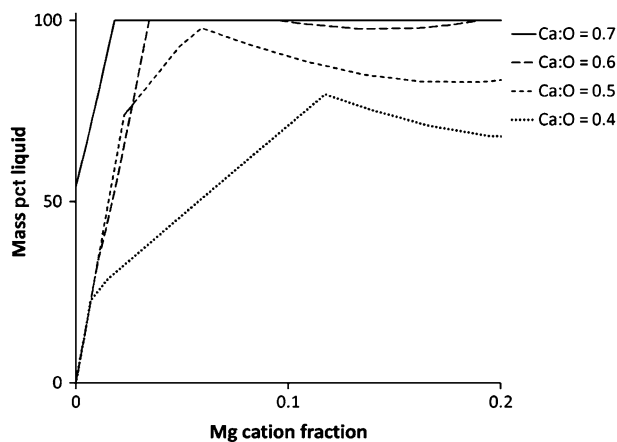


Fig. 2—Percentage of liquid in  $\text{Al}_2\text{O}_3\text{-CaO-MgO}$  inclusions (with different Ca:O mass ratios and  $\text{Mg}/[\text{Mg} + \text{Ca} + \text{Al}]$  cation molar ratios), at 1823 K (1550 °C); calculated with FactSage.

solid in the absence of MgO. As discussed, such a small percentage of MgO may not be detected during the microanalysis of inclusions in polished steel samples.

The strong effect of MgO on liquefaction follows from the  $\text{MgO-Al}_2\text{O}_3\text{-CaO}$  phase diagram directly, as given in Figure 3 (diagram calculated with FactSage, Thermfact/CRCT, Montréal, Canada<sup>[10]</sup>). Small concentrations of MgO, contributing to the liquefaction of calcium-modified inclusions, may help to avoid clogging during industrial casting. For example, Bannenberg showed that slabs with mass ratios of total calcium to total oxygen greater than 0.5 cast successfully.<sup>[11]</sup> Assuming typical values—total oxygen content of 20 ppm, dissolved oxygen content of 4 ppm, and 1 ppm dissolved calcium—the ratio  $\text{Ca}_{\text{tot}}:\text{O}_{\text{tot}} = 0.56$ , much smaller than the mass ratio of Ca:O > 0.7, which is required to achieve largely liquid CaO- $\text{Al}_2\text{O}_3$  inclusions (Figure 2). It seems likely that MgO in the modified inclusions contributed to the successful casting of such slabs.

### C. Reforming Spinels by Reoxidation

Because little calcium (estimated to be around 1 ppm by mass)<sup>[12]</sup> remains in solution in the steel after calcium treatment, subsequent reoxidation of liquid steel would cause unmodified (solid) inclusions to reform. In steel that contained spinels before calcium treatment, magnesium that was returned to the melt during calcium treatment would reform spinels during reoxidation.<sup>[3,13]</sup> The reformation of spinels after reoxidation is illustrated in this study with theoretical calculations and with industrial analyses.

Theoretical calculations were based on the predicted steel compositions after calcium treatment of steel originally containing 0.03 pct Al, 50 ppm S, 4 ppm dissolved oxygen, and 16 ppm bound oxygen (as either  $\text{Al}_2\text{O}_3$  or  $\text{MgAl}_2\text{O}_4$ ), reacted with sufficient calcium to yield liquid inclusions. The calculations were performed with FactSage 6.2, using the FSstel and FToxid databases,<sup>[10]</sup> for a temperature of 1823 K (1550 °C). The predicted liquid steel compositions (after calcium treatment and before reoxidation) are listed in Table I. The steel that contained spinel before calcium treatment had a total (bound) magnesium content of 6 ppm before calcium treatment (for the values assumed in this study); Table I shows that most of this initially bound magnesium was predicted to dissolve in the steel after calcium treatment, giving 4 ppm Mg in solution. This dissolved magnesium would be available to reform spinels during reoxidation. Other magnesium activity data, recently reported by Gran and Sichen,<sup>[14]</sup> imply lower levels of dissolved magnesium (around 1 ppm Mg for the conditions considered in this study); this seems to be too low to account for the practically observed reformation of spinels during reoxidation.

It was assumed that, during subsequent reoxidation, only the dissolved elements in the steel interact with the oxygen with no interaction with the existing oxide inclusions. This assumption was based on the observation (from microanalysis of steel samples) that reoxidized steel often contains two populations of inclusions: the original modified inclusions, together with alumina (or spinel)

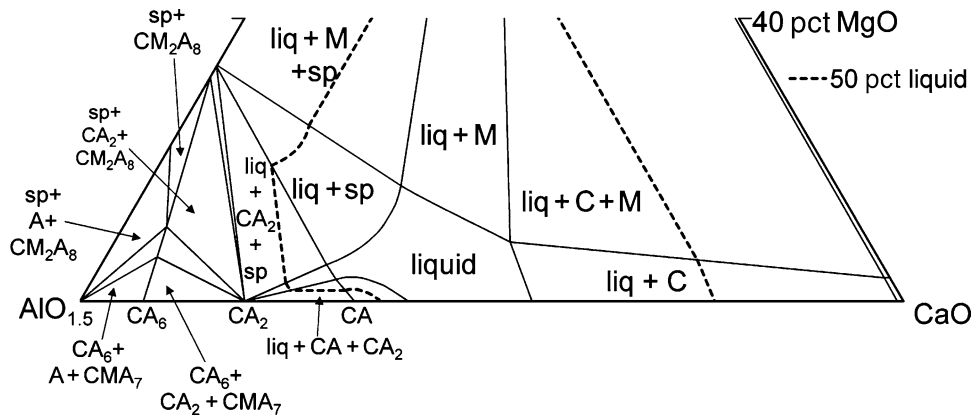


Fig. 3—Partial  $\text{AlO}_{1.5}$ - $\text{MgO}$ - $\text{CaO}$  ternary phase diagram at 1823 K (1550 °C), with dotted 50 pct liquid boundary (compositions plotted as mole fractions of  $\text{MgO}$ ,  $\text{AlO}_{1.5}$ , and  $\text{CaO}$ ); drawn with FactSage. “C” indicates  $\text{CaO}$ , “M”  $\text{MgO}$ , “A”  $\text{Al}_2\text{O}_3$ , and “sp” is spinel solid solution.

**Table I. Calculated Concentrations of Elements in Liquid Steel (Parts Per Million; Mass Basis) after Calcium Treatment of Steel Originally Containing Either Alumina or Spinel Inclusions**

Inclusion Type Before Ca Treatment	Al	O	S	Ca	Mg
Alumina	302	2.0	49.8	1.4	0
Spinel	302	3.6	49.4	1.7	3.9

inclusions (reoxidation products). The results in Figure 4 confirm the expected trend, namely that mainly corundum ( $\text{Al}_2\text{O}_3$ ) inclusions form after reoxidation of the steel, which does not contain dissolved magnesium (with some  $\text{CA}_6$  predicted to form initially by oxidation of the small amount of dissolved calcium). In the steel containing dissolved magnesium (originating from calcium modification of spinel), spinel is predicted to form during initial reoxidation, followed by  $\text{CM}_2\text{A}_8$  (a ternary compound between  $\text{CA}_6$  and spinel) and then corundum.

An analysis of the industrial samples confirmed the latter trend, as illustrated by the inclusion compositions from industrial samples in Figure 5 (redrawn as proportional symbol plots using data previously presented by Lorenzino *et al.*<sup>[15]</sup>). The samples were obtained from the head of cast billet (0.17 m diameter aluminum-killed medium-carbon steel billet, calcium treated before casting). Reoxidation of the steel occurred at the head of the billet, as shown by increases in total oxygen and nitrogen. The billet was sampled at various distances from the head (*i.e.*, zero tons identifies samples taken from the head of the billet, with the most reoxidation; other tonnage values correspond to the distance from the head of the billet to the location of the specific sample). Although the inclusion compositions would have been changed by precipitation and reaction during solidification in the billet, the trend is clear: Spinel inclusions are prevalent in reoxidized steel (closer to the head of the billet). Of the samples showing reoxidation,

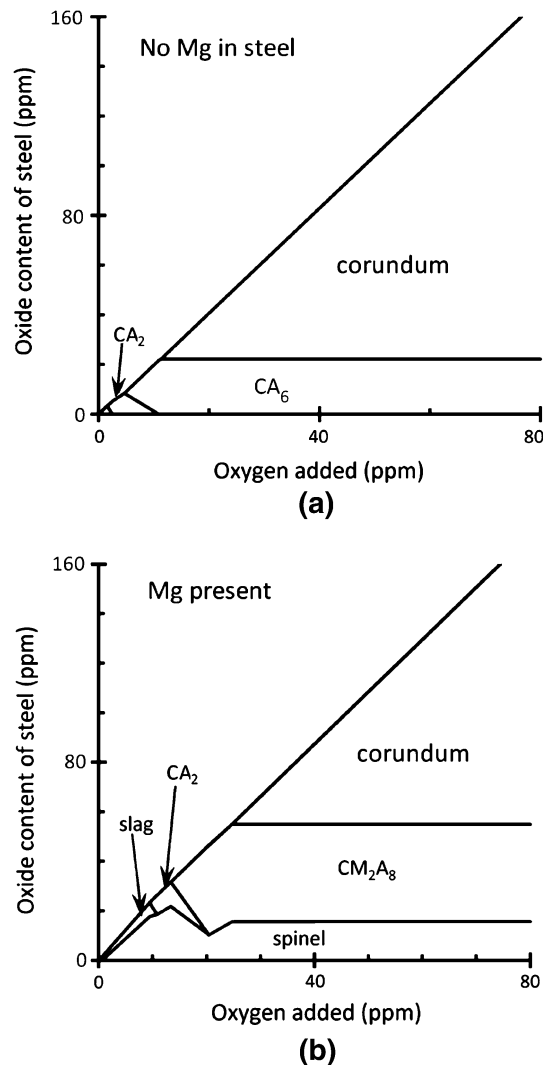


Fig. 4—Predicted composition of inclusions formed by reoxidation of liquid steel, following the calcium treatment of steel that contained (a) alumina and (b) spinel inclusions.

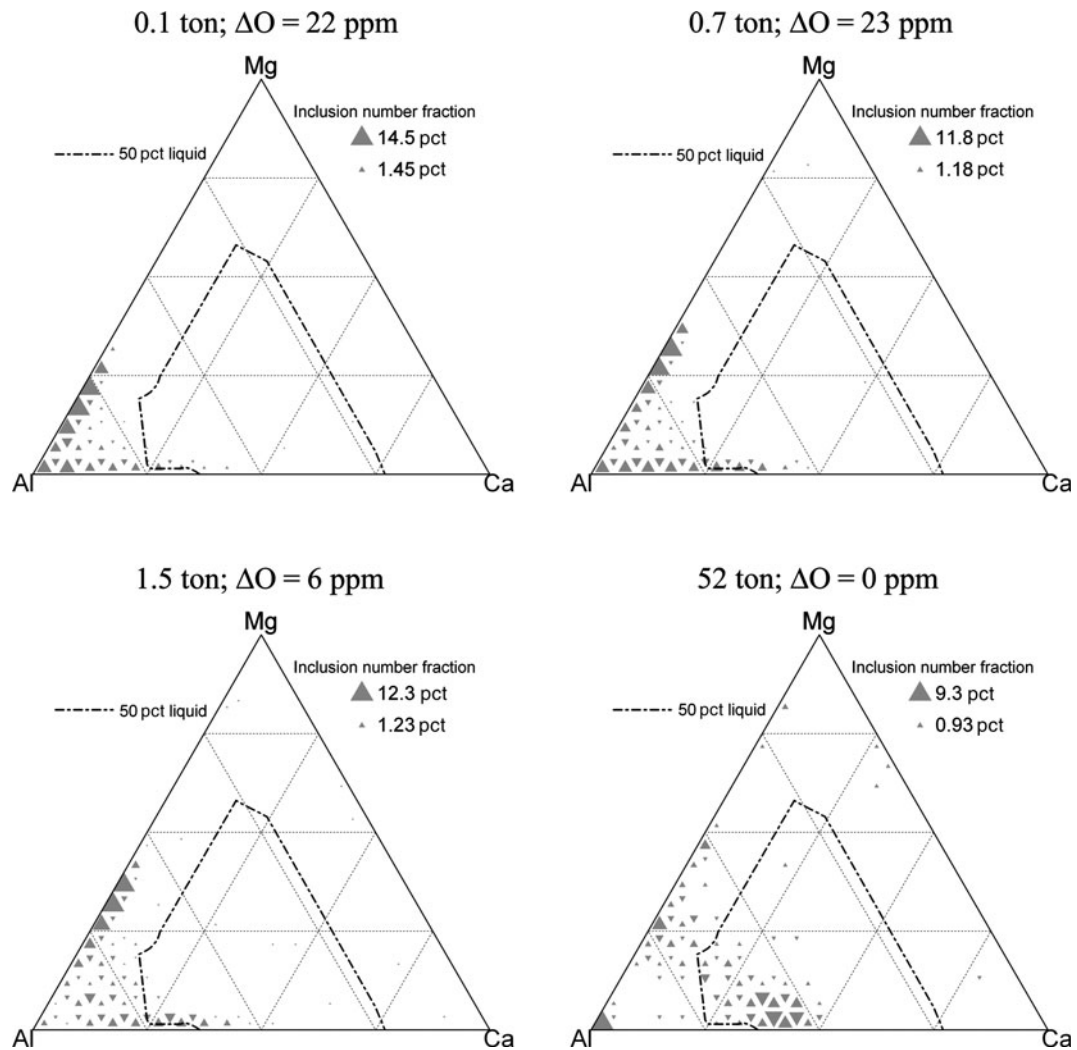


Fig. 5—Change in the distribution of inclusion compositions for the samples recovered at different distances from the head of continuously cast 170-mm round billet (distances expressed as mass of steel cast up to that point). Reoxidation is greater at the smaller masses cast. The increase in total oxygen content relative to the steady state ( $\Delta O$ ) is given for each sample.

the sample with the least reoxidation (1.5 tons steel cast and 6 ppm oxygen pickup) contained mainly spinel inclusions, which is in qualitative agreement with the predictions in Figure 4.

#### D. Questions Addressed in this Work

Even though it is clear from this summary that spinels are modified readily by calcium treatment and that magnesium dissolves in the steel after calcium treatment, some questions remain regarding the reaction mechanism. This article presents results from laboratory and industrial samples to address these questions. The main issues considered in this study are as follows:

- The timing of the decrease in MgO content of spinel inclusions after calcium treatment (previous work indicated that the decrease in MgO occurs not immediately but sometime after calcium treatment<sup>[3]</sup>).
- Whether calcium sulfide plays a similar role in modification of spinels as it does for alumina.

(Recent work has confirmed that CaS is the main reaction product of calcium immediately after calcium injection into aluminum-killed steels containing 40 to 100 ppm sulfur; CaS is subsequently eliminated as alumina is modified.<sup>[16]</sup>)

- Because small percentages of MgO in calcium-modified inclusions affect strongly the degree of liquefaction, the instrumental factors that influence the accuracy of MgO analyses were considered also.

## II. METHODOLOGY

The procedure was the same as described recently, for the study of the modification mechanism of alumina inclusions<sup>[5,8]</sup> and is summarized briefly in this study. Both laboratory and industrial samples were studied using automated and manual scanning electron microscopy (SEM)/energy-dispersive X-ray microanalysis (EDX) to analyze the inclusions detected on polished cross sections. The results from laboratory heats were



presented elsewhere.<sup>[5,13]</sup> In the laboratory heats, spinels were produced by deoxidizing the steel with Al-Mg alloys. Because of the high vapor pressure of magnesium at the liquid steel temperature, magnesium recovery was low, and the extent of spinel formation was variable. Generally, most inclusions were alumina after deoxidation (with some spinels and lower MgO-Al<sub>2</sub>O<sub>3</sub> mixtures). For this reason, laboratory heats were used to study changes in inclusion morphology, using samples from several industrial heats to investigate detailed changes in inclusion composition. The trends in inclusion composition and size were found to be similar in several industrial heats, and the results from one heat are presented in this study.

As described,<sup>[5,8]</sup> the laboratory heats were prepared by induction melting 3 kg high-purity electrolytic iron (12 mm diameter pieces) in an MgO crucible (in an argon atmosphere), deoxidizing with Al-Mg alloys after melting, to produce spinels (3g Al added). The results presented in this article were obtained with Al-15 pct Mg as a deoxidant. Calcium treatment after deoxidation of the steel was performed with 4 g calcium disilicide. Vacuum sampling tubes (7 mm in diameter) were used for sampling of the steel melt, typically 2 minutes after Al-Mg deoxidation and then 2 minutes and 4 minutes after calcium treatment.

Industrial samples were obtained from a plant where vigorous reaction between deoxidized slag and steel (during ladle desulfurization) leads to spinel formation; all the samples were of low-carbon, aluminum-killed steel containing approximately 50 ppm S. Samples were taken before calcium treatment and at various times after calcium treatment.

Three different automated SEM/EDX instruments were used to obtain the analyses presented in this study. The instruments were all operated at 20 kV acceleration voltage with backscattered electron imaging to locate inclusions automatically and using similar EDX detectors to analyze characteristic X-rays. The instruments were the Automated Steel Cleanliness Analysis Tool<sup>[17]</sup> (ASCAT, RJ Lee Group, Monroeville, PA), an ASPEX<sup>[18]</sup> instrument (ASPEX Corporation, Delmont, PA), and a Philips XL30 SEM (FEI, Hillsboro, OR; the latter using INCA software [Oxford Instruments, Oxfordshire, U.K.] to capture and analyze the spectra with the XPP algorithm). Despite the similarity of the instruments, systematic differences in the inclusion compositions obtained with different instruments have been found.<sup>[19]</sup> The differences in the reported composition arise from the inherent difficulty of quantifying the composition of inclusions that are similar in size to the electron-sample interaction volume.<sup>[9]</sup> Typically, 500 to 1000 inclusions were analyzed in each sample; the analyzed inclusions were larger than 1 micron in apparent diameter. The inclusions were also extracted or exposed by full or partial dissolution of the steel matrix in bromine methanol, for subsequent electron microscopy and microanalysis.

Simulated EDX spectra (for oxide inclusions in steel) were calculated with the Monte Carlo package PENEPMA (version 2008) (Universitat de Barcelona, Barcelona, Spain).<sup>[20]</sup>

### III. RESULTS AND DISCUSSION

#### A. Analysis of Magnesium Content of Inclusions

Small but nonzero concentrations of magnesium in calcium-modified inclusions can have a large effect on the proportion of liquid in the modified inclusions at casting temperature (as shown in Figure 2). The magnesium concentration (in inclusions), which is sufficient to make a large difference to the degree of liquefaction after calcium modification, can be so low that it may not be detected during EDX microanalysis. As an example, Figure 6 shows the calculated EDX spectra for hemispherical 1- $\mu$ m diameter inclusions at the surface of steel for two acceleration voltages (20 kV and 10 kV) and for two inclusion compositions: CaO.Al<sub>2</sub>O<sub>3</sub> (“CA”) and a mixture of 97.4 pct CaO.Al<sub>2</sub>O<sub>3</sub> and 2.6 pct MgO (mass basis). The significance of these two compositions is that CA is solid at 1823 K (1550 °C), whereas CA-2.6 pct MgO is fully liquid (Figure 3). The small percentage (2.6 pct) of magnesium oxide, which serves to liquefy the inclusion, gives a small EDX peak; in cases where the EDX quantification software automatically detects the elements to include in composition quantification (using a threshold value of peak height to select elements to quantify), the small height of the magnesium peak may cause magnesium to be excluded from the list of analyzed elements. As Figure 6 indicates, performing the analyses at a lower acceleration voltage—10 kV—would improve the sensitivity for magnesium; this lower acceleration voltage has also been shown to decrease the distorting effect of the steel matrix on the analyzed Ca/Al ratios.<sup>[9]</sup>

To test whether the automatic exclusion of magnesium does affect the analyzed inclusion compositions, the same set of EDX spectra (measured on inclusions in Al-Mg-deoxidized steel using the Philips XL30 instrument) were analyzed using INCA software (Oxford Instruments, Oxfordshire, U.K.), in one case using a fixed list of elements (Fe, Ca, Al, S, Mg, and Mn) and in the other case using the automatic detection of elements to quantify. The results in Figure 7 show that automatic identification resulted in under-reporting of the magnesium content: Where automatic identification caused magnesium to be included in the analysis, the resulting inclusion composition (here represented by the Mg/Al ratio) was essentially the same as when using a fixed list of elements; however, in many cases, the automatic identification caused the magnesium content to be reported as zero. For this specific case, approximately 80 pct of the inclusions were reported to contain zero Mg when using automatic element identification, and only 10 pct when using a fixed element list.

Because the practically important magnesium contents in inclusions are close to the detection level for the EDX microanalysis, the detection of magnesium is expected to depend on the instrument conditions. The instrument factors that increase the likelihood of detecting magnesium include use of a lower accelerating voltage (10 kV rather than 20 kV), obtaining more counts per spectrum (yielding a larger signal-to-noise ratio), and choosing to analyze larger inclusions (thus obtaining more EDX signal from the inclusion itself and

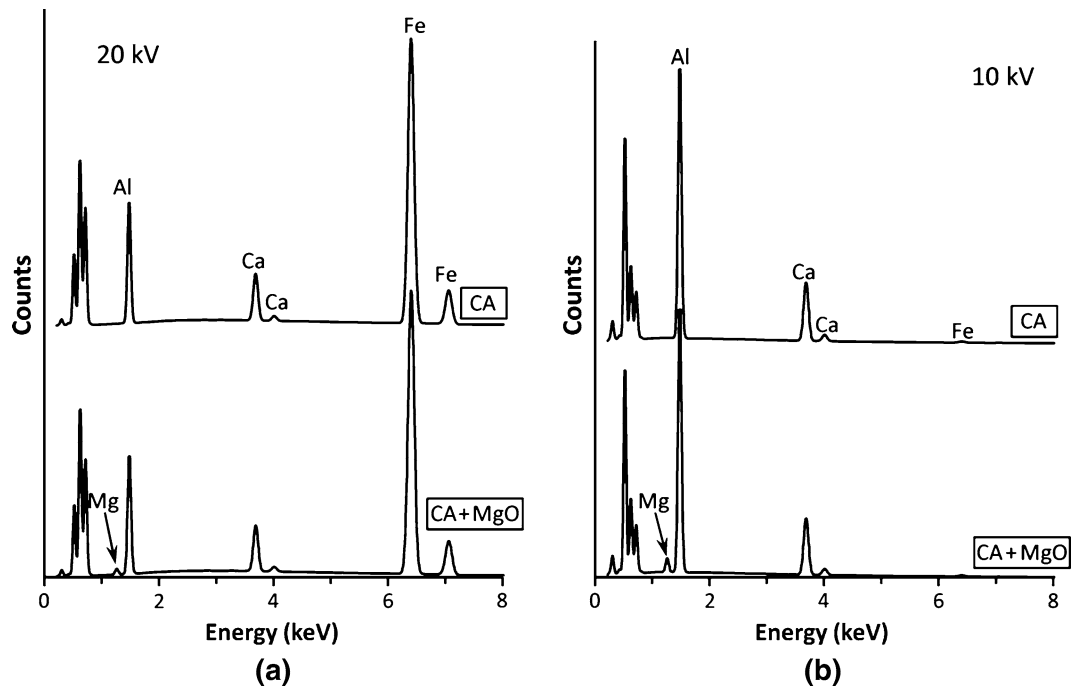


Fig. 6—Calculated EDX spectra from a microanalysis of the hemispherical 1- $\mu\text{m}$  diameter inclusions at the surface of steel. The spectra labeled “CA” are for  $\text{CaO}\cdot\text{Al}_2\text{O}_3$  inclusions (fully solid at casting temperature), and those labeled “CA + MgO” are for a mixture (fully liquid at casting temperature) of  $\text{CaO}\cdot\text{Al}_2\text{O}_3$  (97.4 pct) and MgO (2.6 pct).

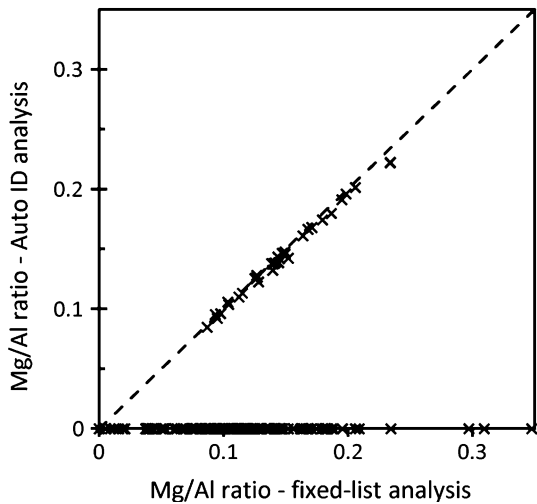


Fig. 7—Effect of mode of quantification of inclusion compositions on the reported Mg/Al ratio. For the same set of EDX spectra, the Mg/Al mass ratio found when using a set list of elements to quantify the inclusion composition is plotted on the  $x$  axis; the Mg/Al mass ratio found when using the automatic element identification feature of the software is on the  $y$  axis.

less from the steel matrix). If magnesium is detected, then the reported composition would also depend on the specific quantification algorithm used by the instrument. Quantifying the composition of micron-sized inclusions—similar in size to the electron interaction volume—is problematic and generally inherently inexact.<sup>[9]</sup> For all these reasons, the reported magnesium content of inclusions can be expected to differ for the measurements performed with different instruments and with the same

**Table II. Comparison of Average Analyses (by SEM/EDX) of Inclusions Detected on Polished Cross Section of an Industrial Steel Sample (Sample Taken 5 Min after Calcium Treatment) and Inclusions Extracted From This Sample by Bromine-Methanol (Molar Percentages)**

Sample	Mg	Al	Ca	S
Polished cross section	0.1	47.4	40.3	12.1
Extracted inclusions	2.6	73.6	23.8	0

instrument at different acceleration voltages or magnifications. As will be shown subsequently, for the samples considered in this article, the ASCAT analyses generally yielded lower magnesium contents in the inclusions than did ASPEX analyses on the same samples.

Under-reporting of MgO in the automated analyses of inclusions exposed on polished cross sections was also confirmed by a comparison with the manual analyses of inclusions extracted (from the same sample) with bromine methanol. EDX spectra from extracted inclusions did not contain the EDX peak from the Fe matrix and, hence, allowed an analysis of lower Mg contents (with the result that a larger proportion of extracted inclusions was reported to have nonzero Mg contents because the Fe signal from the matrix did not diminish the Mg signal to below the threshold). Table II demonstrates that this effect is significant: For the example considered in this article, the extracted inclusions had a Mg cationic fraction of 2.6 pct, whereas the same population of inclusions was reported to have a near-zero Mg cationic fraction when analyzed within the Fe matrix. (The lower Ca and S levels in the extracted inclusions largely resulted from dissolution of CaS by

bromine methanol, and also in part from distortion of EDX analysis at small particle sizes.<sup>[9,21]</sup> An Mg cationic fraction of 2.6 pct is sufficient to make the difference between zero or complete liquefaction (Figure 2), so this difference is indeed significant.

Because of the effect of instrument conditions on the detection of magnesium and the inherent difficulties in quantifying the composition of micron-sized inclusions, magnesium analyses of the inclusions obtained by an EDX microanalysis cannot be taken to be exact. In addition, the analyzed Ca/(Al + Mg) ratio is distorted by the matrix effects,<sup>[9]</sup> and a significant proportion of inclusions is too small to be detected and analyzed by SEM/EDX (in a previous work, the proportion of nondetected inclusions was found to be approximately half to two thirds of oxide and sulfide inclusions by volume, for aluminum-killed steel before and after calcium treatment<sup>[16]</sup>). Despite these significant sources of uncertainty, in this work, some large changes in composition were observed—changes too large to be caused by any analytical artifacts. These composition changes allowed the mechanism of modification of spinel inclusions to be elucidated, as discussed subsequently in this article.

## B. Morphology of Individual Inclusions

### 1. Al-Mg deoxidation products

Figure 8 shows examples (secondary electron images) of MgO-containing inclusions (extracted with bromine methanol) from steel samples taken after Al-Mg deoxidation of laboratory heats. The two kinds of MgO-containing inclusions were pure spinels ( $\text{MgAl}_2\text{O}_4$ - $\text{Al}_2\text{O}_3$  solid solutions; Figure 8(a) and (b)) and low MgO-containing inclusions (with compositions in the spinel + alumina two-phase region at 1873 K [1600 °C]; Figure 8(c) and (d)). It was observed that pure spinels were generally somewhat larger (1  $\mu\text{m}$  to several microns), whereas low-MgO inclusions were usually below 1  $\mu\text{m}$ . Agglomerated spinels were also observed; an example is shown in Figure 8(e). Apart from these MgO-containing inclusions, pure alumina inclusions were observed also (and constituted the majority of inclusions in the laboratory heats).

### 2. Inclusion morphology after calcium treatment

Various inclusion morphologies were obtained after calcium treatment; most inclusions were heterogeneous in composition. Examples of EDX element maps of such

inclusions have been presented elsewhere<sup>[4]</sup>; typical morphologies are shown in Figure 9 and described briefly subsequently.

*a. Immediately after calcium treatment: CaS adhering to alumina and unmodified or partially modified spinel.* As in the case of calcium-treated alumina inclusions,<sup>[16]</sup> transient CaS-containing inclusions were observed in the case of spinel modification as well. Spinel-CaS combinations were observed rarely; the major transient state of the inclusion observed was  $\text{Al}_2\text{O}_3$ -CaS combinations.

*b. Longer after calcium treatment: Fully and partially modified spinels.* Partially modified spinels are expected to be two-phased mixtures of unreacted spinel and low-MgO liquid at temperature (based on the phase diagram, Figure 3); such combinations were observed commonly. Where more calcium had reacted with an inclusion, the inclusions were modified by calcium uniformly and usually were globular in shape.

Figure 10 shows the inclusion size distributions (based on inclusion counts) for the various samples taken from the industrial heat. The size distribution changed after calcium injection, shifting to smaller sizes (in sample L2—taken immediately after calcium treatment—and sample L3, taken 5 minutes after calcium treatment). Some agglomeration of inclusions seemed to have occurred for the tundish sample, in which the inclusions are somewhat larger than in the L2 and L3 samples. This decrease in inclusion size soon after calcium treatment was also observed in laboratory heats (not shown in this study). Because many inclusions were in the size range 1 to 2.5  $\mu\text{m}$  in these samples and the size cutoff for automated analyses was 1  $\mu\text{m}$ , some inclusions were undoubtedly smaller than this and were not detected and not included in the analysis. It is likely that this result is the origin of the apparent increase in inclusion content from before calcium treatment to the tundish (as indicated by the increased inclusion areas reported in Table III), and it is in line with analysis of calcium-modified alumina inclusions.<sup>[16]</sup>

## C. Inclusion Compositions

The inclusions were found to contain Ca, Al, Mg, and S (and oxygen); no significant Mn was detected. When considering the calcium modification of alumina inclusions in the S-containing steel, it was found sufficient to display the inclusion compositions on ternary plots

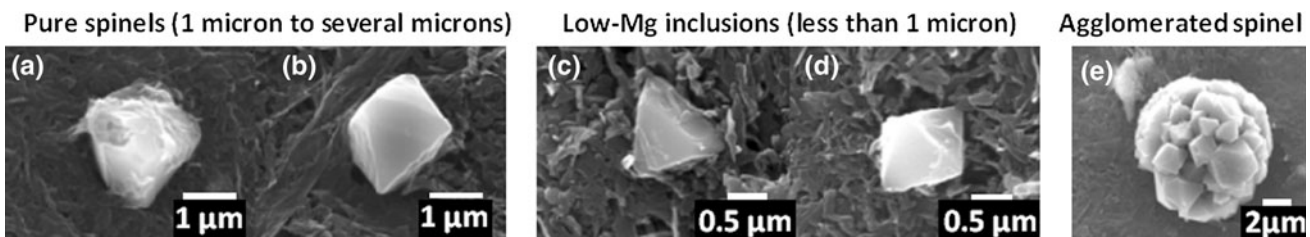


Fig. 8—Secondary electron images of extracted inclusions (Mg-containing inclusions after Al-Mg deoxidation).



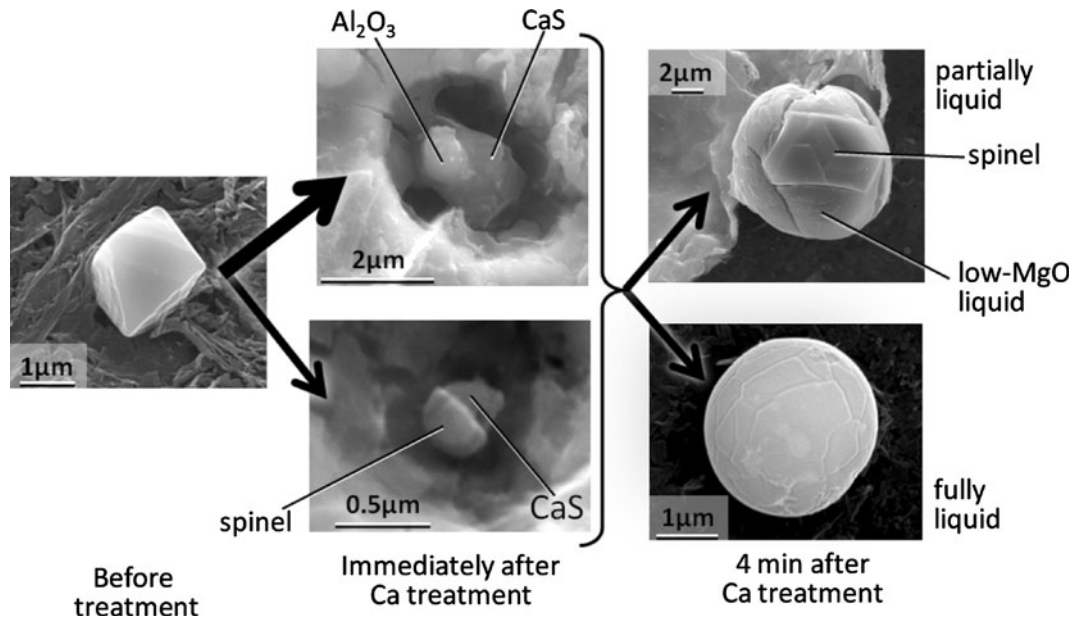


Fig. 9—Typical inclusion morphologies after deoxidation and after calcium treatment.

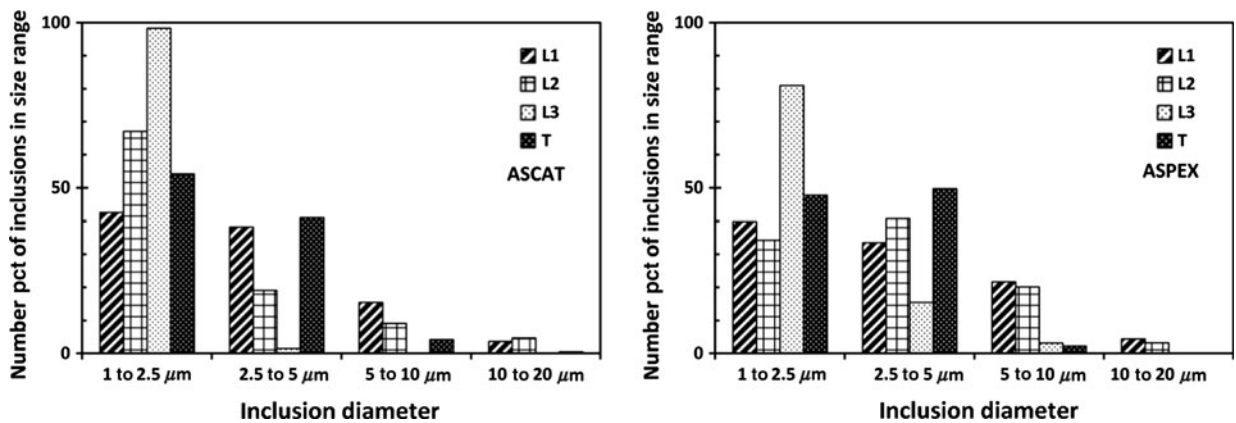


Fig. 10—Size distributions (based on inclusion counts) of the inclusions detected in the polished cross sections of samples taken at various times from an industrial heat (inclusions analyzed by ASCAT and ASPEX). L1: before Ca treatment; L2: immediately after calcium treatment; L3: 5 min after calcium treatment; T: tundish sample.

(of Al, Ca, and S).<sup>[7]</sup> In the results presented in this article, three ternary diagrams were projected from each set of analyses (see Figures 11 through 13), to visualize changes in the relative amounts of Ca, Al, Mg, and S. In each ternary diagram, the inclusion compositions are normalized to 100 pct with respect to the elements in the plot: To draw the Ca-Al-S plots, Mg was deleted from the inclusion compositions; in the Ca-Al-Mg plots, CaS was subtracted to show the oxidic part of the inclusions; and in the Mg-Al-S plots, Ca was subtracted to show a possible association between magnesium-containing inclusions and sulfur. For clarity, only one Mg-Al-S plot is shown (in Figure 13). In the Ca-Al-S and Ca-Al-Mg plots, the broken lines indicate the 50 pct liquid boundaries. However, these boundaries are exact only if the inclusions consist of only the three elements (plus oxygen) plotted on that diagram; in reality, small concentrations of MgO in CaS-CaO-Al<sub>2</sub>O<sub>3</sub> inclusions increase the liquid region considerably (as suggested by

**Table III. Average Compositions (Molar Percentages; First Number Is ASCAT Analysis and Second Number Is ASPEX Analysis) of Inclusions Detected in Industrial Steel Samples**

	Mg	Al	S	Ca	Area (ppm)
L1	17/25	74/62	2/2	7/10	75
L2	4/7	50/60	18/9	27/23	70
L3	0.4/4	40/36	23/17	37/43	110
T	0.3/4	59/46	7/10	34/40	170

Figure 2); also—as discussed in this article—the inclusion compositions cannot be quantified exactly. Hence, the 50 pct liquid boundaries give only an approximate indication of the inclusion liquefaction.

The samples from six industrial heats were examined, but these all showed similar effects and, hence, detailed analyses from only one heat are presented in this article. The same trends were observed in the laboratory and



industrial samples: The MgO content of the inclusions decreased immediately after calcium treatment (and in the industrial samples, it decreased even more with time in the ladle; see Table III). Calcium sulfide was evident immediately after calcium treatment and then decreased over time as calcium aluminates (modified inclusions)

formed. These shifts in composition are evident in the inclusion composition distributions shown in Figures 11 and 12. Although differences in the magnesium contents are found with ASCAT and ASPEX analyses (see also Table III), the qualitative trends are the same in

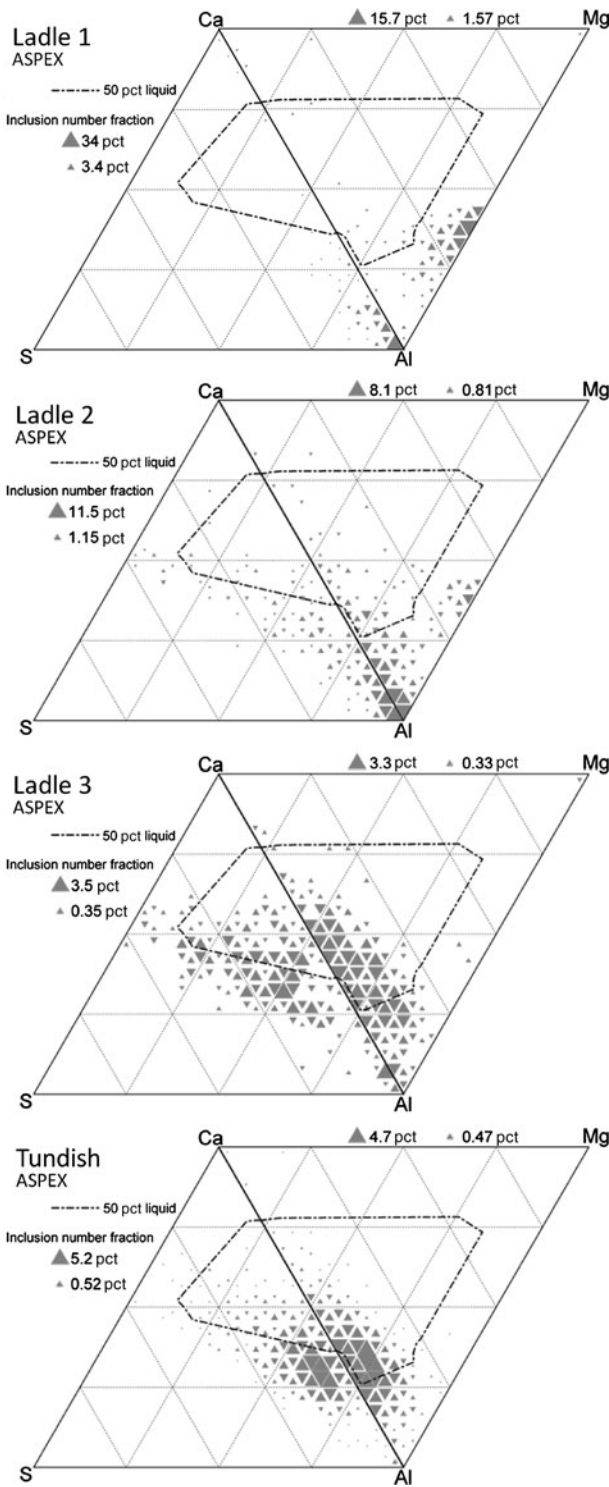


Fig. 11—Inclusion compositions as found in samples from an industrial heat, analyzed with ASPEX. See Fig. 10 for explanation of designations ladle 1 to 3 (L1 to L3) and tundish (T).

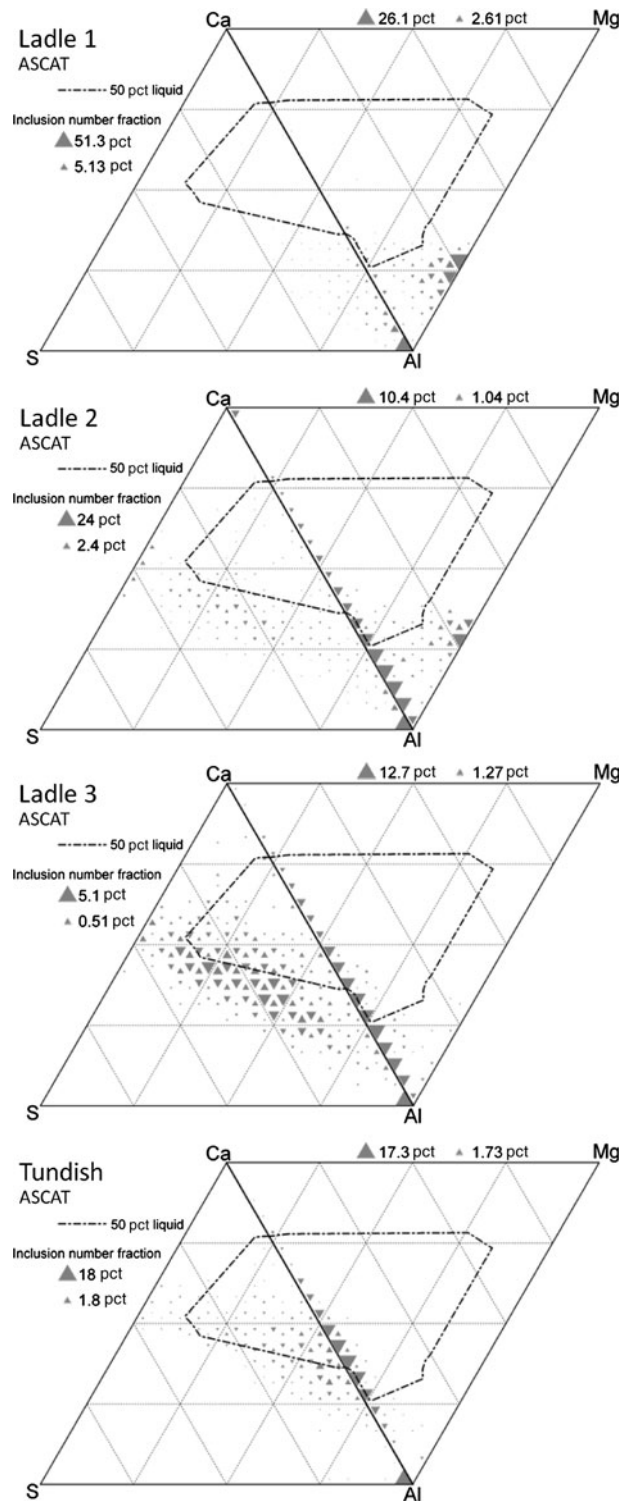


Fig. 12—Inclusion compositions as found in the samples from an industrial heat, analyzed with ASCAT (same heat as in Fig. 11); see Fig. 10 for explanation of designations ladle 1 to 3 (L1 to L3) and tundish (T).

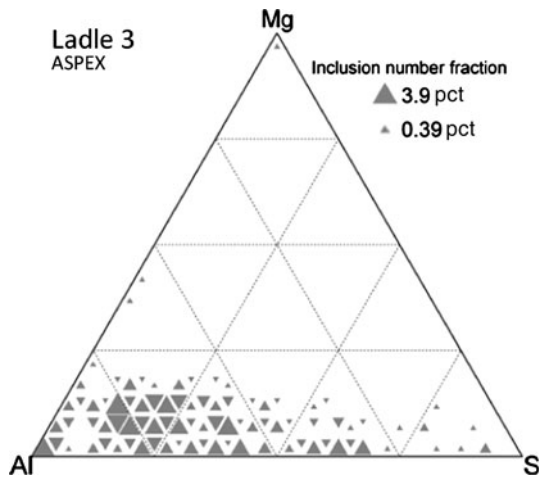


Fig. 13—Composition of inclusions in the ladle 3 sample from an industrial heat, analyzed with ASPEX, showing Al-Mg-S ternary projection (Ca deleted from analyses) (same heat and analyses as in Fig. 11).

Figures 11 and 12: The inclusions included mainly spinels (plotting along the Al-Mg join in the Ca-Mg-Al diagram, sample ladle 2) before calcium treatment. Immediately after calcium treatment, a few spinel inclusions remained, but most inclusions were  $\text{Al}_2\text{O}_3$  with a small proportion of CaO, and associated with CaS (as shown by the Ca-Al-S diagram for sample ladle 2). Little sulfur was associated with the remaining spinel inclusions, as shown by the spinel compositions plotting close to the Mg-Al join in the Mg-Al-S diagram (Figure 13). These composition distributions agree with the trend based on an observation of many individual inclusions and summarized in Figure 9: Immediately after calcium treatment, the dominant inclusion type was alumina with associated CaS, together with a small proportion of spinels with CaS.

The proportion of detected CaS inclusions increased relative to the oxide inclusions in the sample taken 5 minutes after calcium treatment (ladle 3). This increase probably resulted from the small size of CaS immediately after calcium treatment (inclusions smaller than 1 micron in apparent diameter were not analyzed), and it suggests that the calcium sulfide nucleated in the liquid steel rather than on the spinel inclusions. (If the calcium sulfide had nucleated on the spinel inclusions, then calcium sulfide would have been detected after an EDX analysis of the oxide inclusions.)

With the subsequent passage of time, calcium sulfide was consumed and the Ca/Al ratio in the oxide inclusions increased; calcium sulfide, hence, plays a similar role in modification of spinel inclusions as it does in the modification of alumina.<sup>[16]</sup>

#### 1. Decrease in MgO content

Inclusions in industrial samples had high Mg contents before calcium treatment (averaging 15 to 20 mol pct in ASCAT analyses and somewhat higher for ASPEX; see Table III, sample L1). After calcium treatment (L2 and L3 in Table III), the Mg contents of the inclusions decreased sharply. Taken together with the reappearance of MgO-containing inclusions after the reoxidation

of laboratory<sup>[13]</sup> and industrial<sup>[3]</sup> heats (see also Figure 5), these changes support the suggestion that magnesium dissolves in the steel after calcium treatment (as also predicted by equilibrium calculations; Table I).

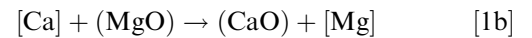
Overall, the industrial samples confirmed the sharp decrease of MgO content of inclusions immediately after introduction of calcium, as in laboratory heats. The major part of the decrease in MgO was observed immediately after Ca treatment, but CaS persisted for much longer. Thus, the MgO from the spinel was largely reduced before CaS-based modification of the oxide inclusions started.

#### D. Proposed Mechanism for Spinel Modification

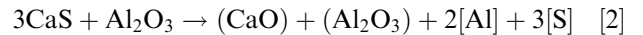
Figure 9 summarizes the observed modification route of spinel inclusions, involving transient CaS formation and preferential reduction of MgO (thus resulting in a low MgO content in modified inclusions).

Based on these observations, the following modification mechanism is proposed:

Injected calcium (as vapor or dissolved calcium) reacts with dissolved sulfur to form CaS and reduces MgO from the spinels



CaS reacts with the oxide (mainly  $\text{Al}_2\text{O}_3$ ) inclusions, returning sulfur to the melt.



According to this mechanism, the second step (reaction between CaS and  $\text{Al}_2\text{O}_3$ ) is identical to that proposed for modification of alumina,<sup>[16]</sup> with no apparent role of MgO in this reaction. The importance of the low but significant remaining concentration of MgO in the modified inclusions is the large effect of MgO on liquefaction (Figure 2) and, hence, castability.<sup>[3]</sup>

## IV. CONCLUSIONS

Successful modification of  $\text{MgO-Al}_2\text{O}_3$  spinels to liquid or partially liquid state by calcium treatment was demonstrated with laboratory and industrial samples. As in the case of alumina, the modification of spinel inclusions proceeded through a transient CaS formation. MgO was observed to be reduced preferentially from the spinels during calcium modification, resulting in magnesium dissolved in the steel at ppm concentrations. Should reoxidation occur, the dissolved magnesium would form fresh spinels that can lead to clogging.

## ACKNOWLEDGMENTS

Support of this work by the industrial members of the Center for Iron and Steelmaking Research (CISR) is acknowledged gratefully.

## REFERENCES

1. K.C. Ahlborg: *Fifth Int. Conf. on Clean Steel*, OMBKE, Budapest, Hungary, 1997, pp. 151–56.
2. S.R. Story, S.M. Smith, R.J. Fruehan, G.S. Casuccio, M.S. Potter, and T.L. Lersch: *Iron Steel Technol.*, 2005, vol. 2 (9), pp. 41–49.
3. E.B. Pretorius, H.G. Oltmann, and T. Cash: *Iron Steel Technol.*, 2010, vol. 7 (7), pp. 31–44.
4. S.R. Story, F.J. Mannion, G.S. Casuccio, and M.S. Potter: *Proc. of the Richard J. Fruehan Symposium, Physical Chemistry of Sustainable Metals*, AIST, Pittsburgh, PA, 2011, pp. 403–22.
5. N. Verma, M. Lind, P.C. Pistorius, and R.J. Fruehan: *Iron Steel Technol.*, 2010, vol. 7 (7), pp. 189–97.
6. P.C. Pistorius, P. Presoly, and K.G. Tshilombo: *Sohn Int. Symp., Advanced Process. of Metals and Materials*, vol. 2, TMS, Warrendale, PA, 2006, pp. 373–78.
7. S. Yang, J. Li, Z. Wang, J. Li, and L. Lin: *Int. J. Miner., Metall. Mater.*, 2011, vol. 18, pp. 18–23.
8. N. Verma, P.C. Pistorius, R.J. Fruehan, M. Potter, M. Lind, and S. Story: *Metall. Mater. Trans. B*, 2011, vol. 42B, pp. 711–19.
9. P.C. Pistorius and N. Verma: *Microsc. Microanal.*, 2011, vol. 17, pp. 963–71.
10. C.W. Bale, P. Chartrand, S.A. Degterov, G. Eriksson, K. Hack, R. Ben Mahfoud, J. Melançon, A.D. Pelton, and S. Petersen: *CALPHAD: Comput. Coupling Phase Diagrams Thermochem.*, 2002, vol. 26, pp. 189–228.
11. N. Bannenber: *Steelmaking Conf. Proc.*, 1995, vol. 78, pp. 457–63.
12. Y. Kang, F. Li, K. Morita, and D. Sichen: *Steel Res. Int.*, 2006, vol. 77, pp. 785–92.
13. N. Verma, P.C. Pistorius, R.J. Fruehan, M. Lind, H. Oltmann, E. Pretorius, and M. Potter: *AISTech 2011 Conf. Proc.*, vol. II, Association for Iron & Steel Technology, Warrendale, PA, 2011, pp. 607–15.
14. J. Gran and D. Sichen: *Metall. Mater. Trans. B*, 2011, vol. 42B, pp. 921–24.
15. P. Lorenzino, C. Capurro, C. Cicutti, P. Lardizabal, G. Torga, and F. Fuhr: *17th IAS Steelmaking Conf.*, Campana, Buenos Aires, Argentina, 2009, pp. 223–32.
16. N. Verma, P.C. Pistorius, R.J. Fruehan, M. Potter, M. Lind, and S. Story: *Metall. Mater. Trans. B*, 2011, vol. 42B, pp. 720–29.
17. S.R. Story, T.J. Piccone, R.J. Fruehan, and M.S. Potter: *Iron Steel Technol.*, 2004, vol. 1 (9), pp. 163–69.
18. F. Schamber: *Introduction to Automated Particle Analysis by Focused Electron Beam*, <http://www.aspexcorp.com>, 2011.
19. N. Verma, P.C. Pistorius, R.J. Fruehan, and M. Lind: *AISTech 2011 Proc., Vol. II, Association for Iron & Steel Technology*, Warrendale, PA, 2011, pp. 627–34.
20. F. Salvat, J.A. Escuder, D. Bote, and X. Llovet: *Microsc. Microanal.*, 2007, vol. 13, pp. 1388–89.
21. J.T. Armstrong and P.R. Buseck: *Anal. Chem.*, 1975, vol. 47, pp. 2178–92.